A Real-Time Close-Range Imaging System with Fixed Antennas

Birgit Michael, Wolfgang Menzel, *Senior Member, IEEE*, and Arnold Gronau

***Abstract*—A coherent system with two stepped frequency radar sensors separated by 1–2 m is presented in this paper for close-range imaging. Resolution is achieved via range resolution from the two different sensor positions, exploiting both monostatic and bistatic responses. A first test had been performed using a vector measurement equipment for an antenna measurement range as a radar simulator, and now, a mobile experimental system was built and tested, which included stationary and mobile targets.**

***Index Terms*—Doppler radar, FM radar, microwave imaging, radar imaging.**

I. Introduction

IMAGING OF different scenes, even under adverse environmental conditions, is playing an important role for a number of applications like autonomous vehicles (robots) or as a collision warning for cars driving forward or backward or changing lanes [1]–[6]. In a number of these scenarios, an imaging of the relevant area around the vehicle has to be performed. In most cases, this is done by a scanning antenna with a narrow beamwidth in azimuth [4], [5]. This, however, requires antennas with relatively large lateral dimensions combined with mechanical [4] or electronic scanning, e.g., frequency scanning [5], resulting in large and expensive antenna arrangements. For close-range imaging, on the other hand, an imaging is also possible by performing separate measurements from at least two different positions via range, using wide-beamwidth antennas. Therefore, a novel system for close-range imaging was proposed using two antennas separated by 1–2 m [7]. In the meantime, a mobile experimental radar system has been built and tested. The original imaging algorithms have been extended to detect and correctly determine both location ***and*** speed of the moving targets.

II. Imaging Principle

The proposed arrangement consists of two radar sensors separated by approximately the width of the respective vehicle. The antennas have a wide beamwidth in azimuth, whereas a narrower beamwidth typically is desirable in elevation. To this end, H-plane waveguide horns including a lens for reduced length with horizontal polarization and beamwidths of 77° in azimuth and 12° in elevation and a gain of 16 dBi were employed. For a single target, each sensor gives a monostatic, as well as a bistatic, response according to the respective distance; taking into account reciprocity, three independent sets of data are available for each target, which are represented by two circles around each antenna and an ellipse with the antennas as focal points (Fig. 1).

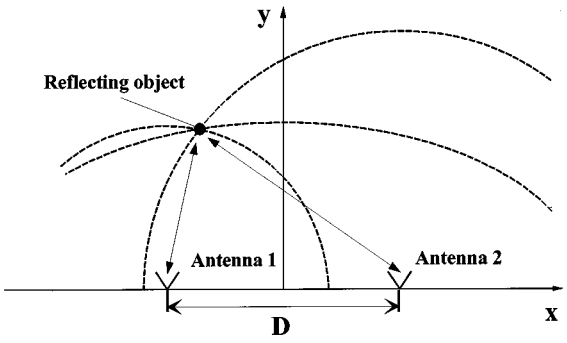

Fig. 1. Basic principle of the imaging sensor.

This already gives some means to separate multitarget scenarios; this can be improved considerably by employing a coherent sensor system. For system simplicity and for minimal effective isotropic radiated power (EIRP), frequency-modulated continuous wave (FMCW)—or stepped frequency sensors—are advantageous. For a stepped frequency system, a coherent evaluation of the measured data can be done by multiplying the responses of the three measurements

$$A(P) = \left(r_{1P} \sum_{i=0}^{N-1} \boldsymbol{E}_{i11} \cdot e^{j2k_i r_{1P}} \right) \cdot \left(r_{2P} \sum_{i=0}^{N-1} \boldsymbol{E}_{i22} \cdot e^{j2k_i r_{2P}} \right) \cdot \left(\sqrt{r_{1P} \cdot r_{2P}} \sum_{i=0}^{N-1} \boldsymbol{E}_{i12} \cdot e^{jki(r_{1P}+r_{2P})} \right) \quad (1)$$

where $A(P)$ is the amplitude from a possible target at point P and E_{i11} and E_{i22} are the received electric fields at frequency step i at antennas 1 and 2, respectively, transmitted by the same antenna. The third term of this equation represents the bistatic response; E_{i12} could equally be replaced by E_{i21} due to reciprocity. r_{1P} and r_{2P} are the distances between antennas 1 and 2 and the target. In the range close to the radar system, the arrangement is nearly two-dimensional; thus, for a range-dependent amplitude correction, a dependence of the electric field as $1/r$ is assumed. The summation in (1) is done over the number N of measured frequency points. The overall measurement bandwidth Δf determines the sensor resolution $\Delta R = c_0/(2\Delta f)$, while N determines the unambiguous range of the sensor system $R_{unamb} = N \cdot \Delta R$.

Manuscript received February 21, 2000; revised August 25, 2000.

B. Michael is with DaimlerChrysler Research, D-89013 Ulm, Germany.

W. Menzel and A. Gronau are with the Department of Microwave Techniques, University of Ulm, D-89069 Ulm, Germany.

Publisher Item Identifier S 0018-9480(00)10796-3.

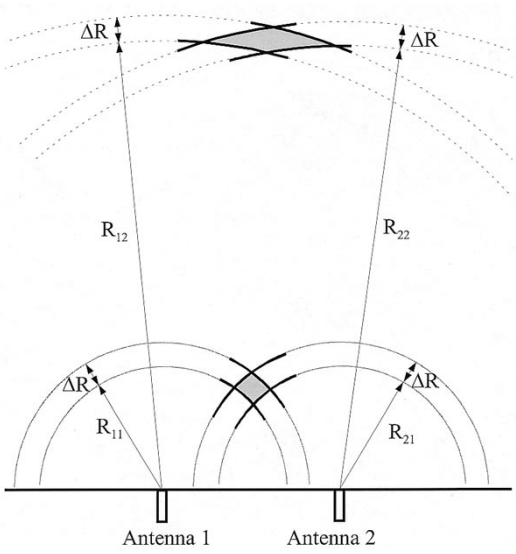

Fig. 2. Resolution cells for close range (bottom) and far range (top) targets.

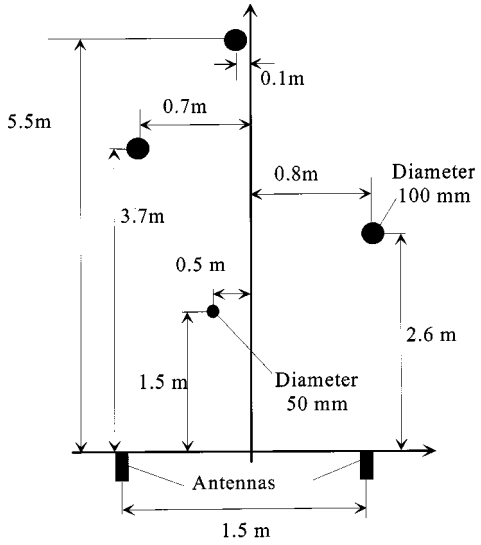

Fig. 3. Geometrical arrangement of four metal cylinders.

Possible frequencies of operation of such sensors may be around 24, 61, or 77 GHz. For the test system described here, 24 GHz was chosen.

In Fig. 2, the two-dimensional resolution of the measurement system is demonstrated for two different targets: one close to the sensor and another one further away. As the circles indicating the range resolution intersect at large angles for the close-range target, a good longitudinal, as well as a good lateral resolution, is achieved. For targets further away, the range circles intersect at flat angles. A good longitudinal resolution is maintained, associated, however, with an increasingly wider response in the lateral dimension (Fig. 2).

III. Stationary Measurements

Using a vector-network analyzer as measurement system and offline data processing, preliminary tests with varying bandwidths and with up to 801 frequency points have been made.

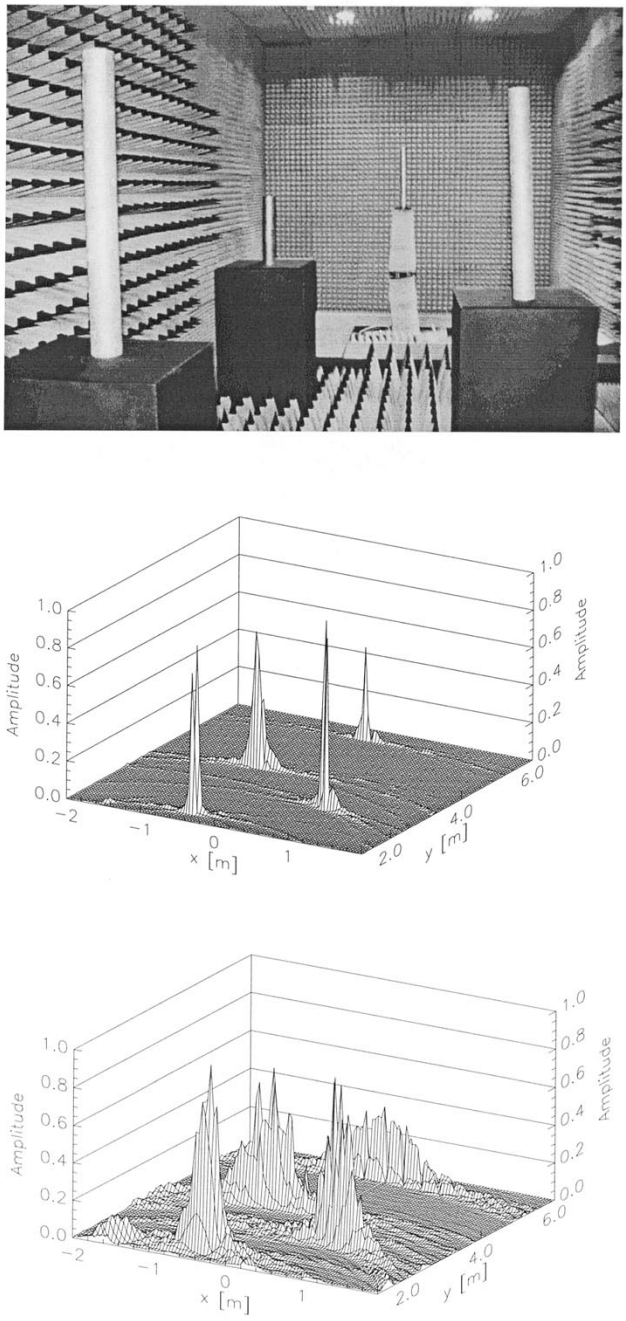

Fig. 4. Photograph and radar images of a four-cylinder arrangement according to Fig. 2 recorded with bandwidths of 11 (top) and 1 GHz (bottom).

A first arrangement consisting of four metal cylinders is shown in Figs. 3 and 4.

The related radar image taken in an antenna range is plotted in Fig. 4 for an 11- as well as 1-GHz bandwidth. The arrangement of the targets can be clearly recognized. For increasing distance, the displayed target width is increased, as discussed before.

Another test was done in an open environment, as shown in Fig. 5 (top). The grassy ground is a much more severe clutter environment. Radar results at both 11- (middle) and 1-GHz (bottom) bandwidth are plotted in Fig. 5. The 1-GHz data were evaluated using a Tukey windowing technique [8], resulting in a much better visibility of the two target cylinders.

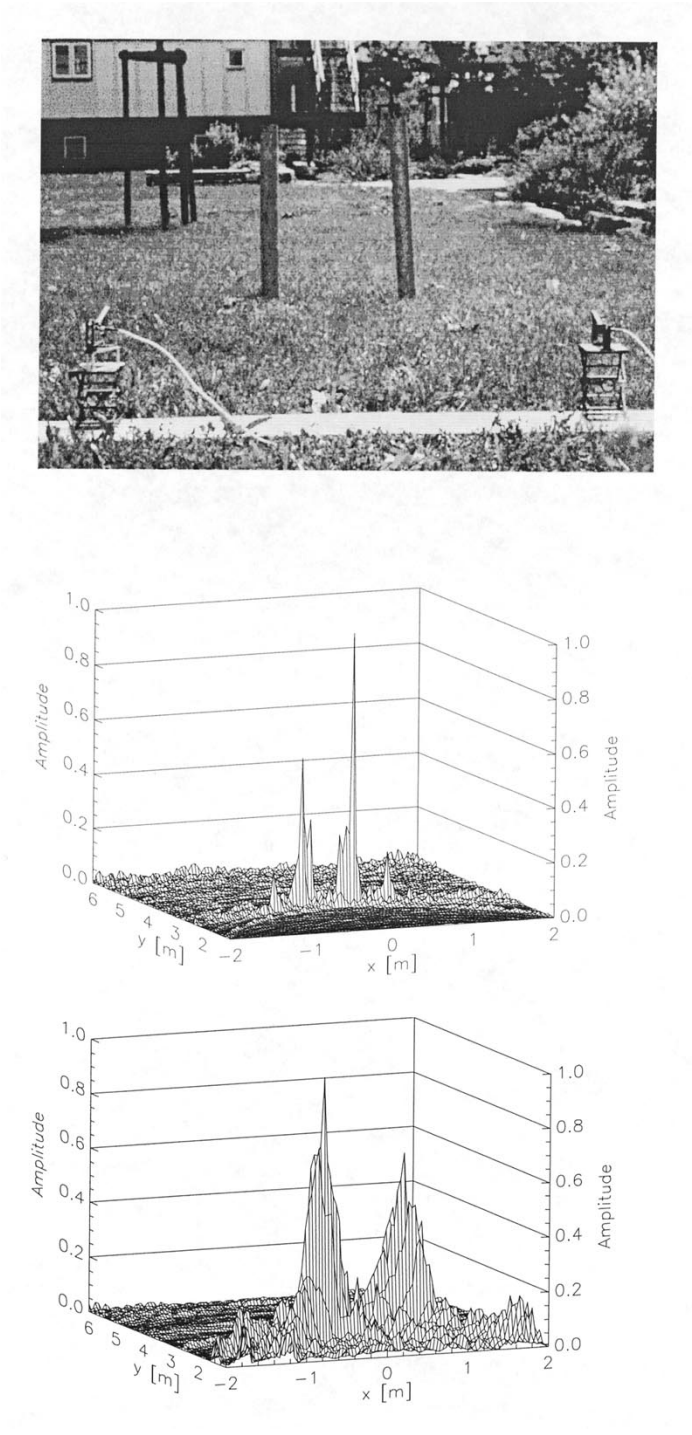

Fig. 5. Photograph (top) and radar images of a two-cylinder arrangement according to a grassy ground recorded with bandwidths of 11 (middle) and 1 GHz (bottom).

With this standard network analyzer equipment, however, acquisition time is rather long—about 30 s for a single-frequency ramp with 801 points (step mode); therefore, only measurements of static targets close to the laboratory could be done.

IV. Mobile Real-Time Sensor System

To evaluate the imaging principle presented above in arbitrary scenarios and including realistic, e.g. moving, targets, an experimental system was built and tested. A block diagram of the radar sensor is given in Fig. 6. Separate antennas were used for transmit and receive to improve transmit–receive isolation, and a bandwidth of 500 MHz (24–24.5 GHz) was chosen as a compromise between resolution, possible postal restrictions, and effort. Part of the components use commercially available parts; others, like filters or mixers, were designed and fabricated for this application using planar techniques. Consequently, the present system is still rather complex and bulky; it could be made much more compact and cheaper for an operational system.

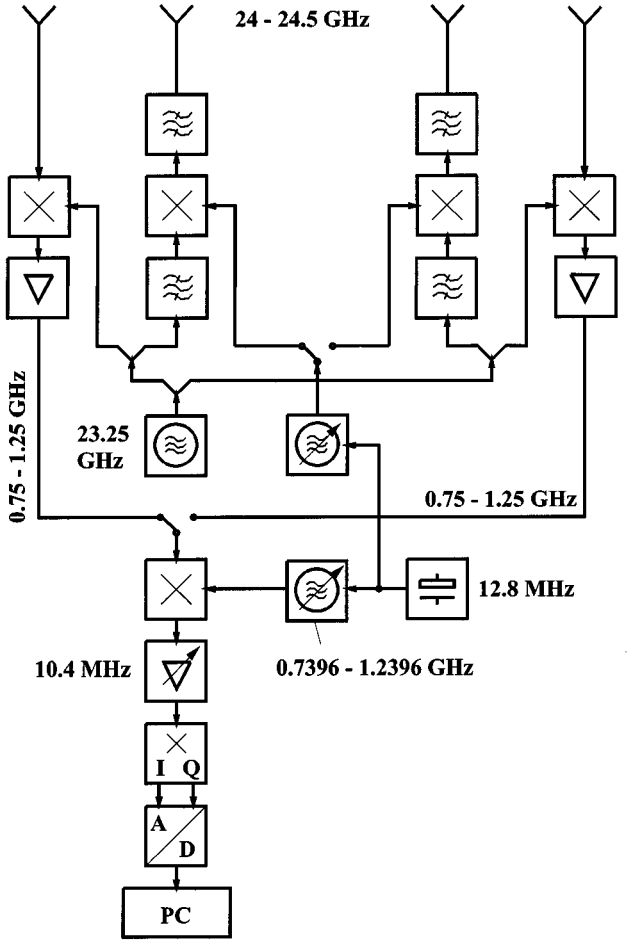

Fig. 6. Block diagram of the real-time mobile radar sensor.

The test system was built in two separate blocks. The first one consists of the RF part with the antennas; these are mounted on a carrier system, which can then be mounted in front of a test vehicle. IF circuits, control, signal processing, and power supply are arranged in a rack and connected to the RF part by a cable of sufficient length to place this part into the interior of the vehicle.

Operation of the system is controlled by an integrated PC. This PC, at the same time, stores the data and does a first evaluation of the radar image. A detailed analysis of the data, however, is done offline later on.

Output power of the radar at the antennas is limited to approximately -27 dBm only, and the receiver noise figure to 15 dB. For each measurement cycle, 128 frequencies are adjusted for both monostatic and bistatic measurements. Switching between

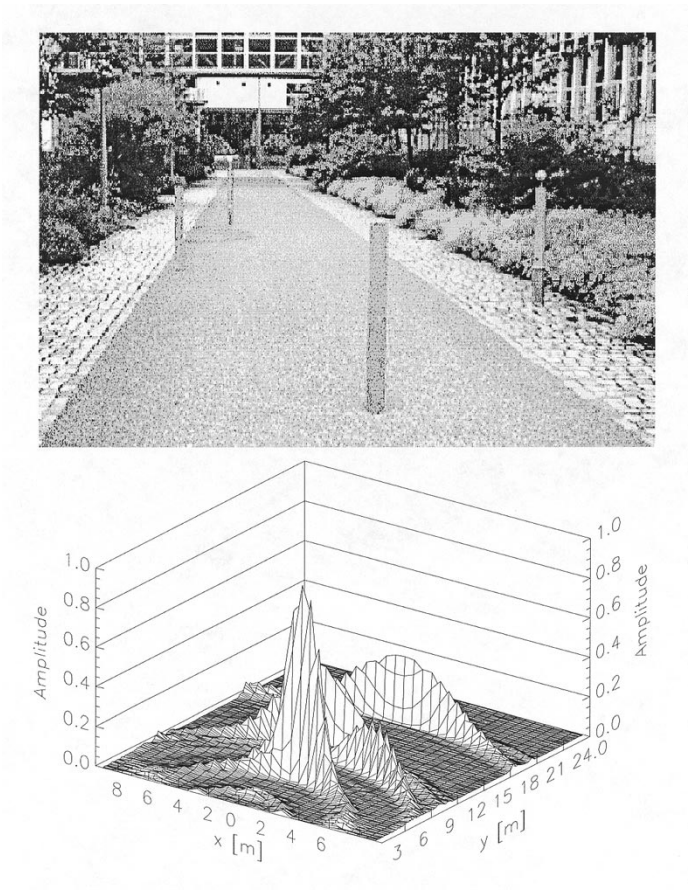

Fig. 7. Photograph and radar image of a four-post scene.

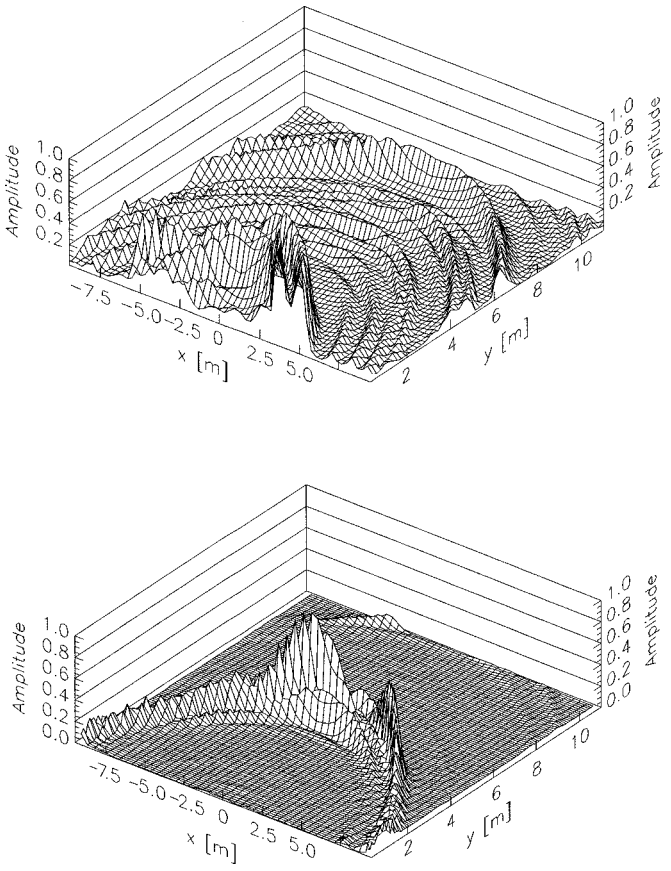

Fig. 8. Radar image of a moving car (top: uncorrected data, bottom: Doppler corrected data according to (2) [speed 1.5 m/s, distance 5.5 m]).

antennas or frequencies takes about 210 μs for the filters to settle. Data acquisition time is 10 μs (from the AD converter). With eight samples per frequency, one frequency ramp, therefore, takes about 38 ms.

A first test of this system was done in a stationary environment, i.e., Fig. 7 (top). The resulting radar image is displayed in Fig. 7 (bottom). The four posts situated on a small road can be recognized easily in the radar image. With increasing distance, the displayed widths of the targets get wider, as discussed in Section II. Nevertheless, even at a distance of over 18 m, the last post can be identified clearly.

V. Evaluation of Moving Targets

To include moving targets, two steps were taken. The own speed of the vehicle with the radar sensor typically is known; a respective Doppler frequency correction can easily be included into the image processing. A more complex task is the detection of both speed (absolute value and direction) and location of an independently moving target within the imaging range.

Without any additional processing, a rather disturbed image of a moving car results, as shown in Fig. 8 (top). To solve this problem, the signal-processing algorithm is modified. In a first step, a number of measurements are done at a single frequency, from which the radial Doppler frequencies are determined with respect to the monostatic and bistatic responses. (As a further improvement, the extraction of the Doppler information from the frequency-stepped mode will be investigated, e.g., by alternatively using increasing and decreasing frequency ramps.) The normal stepped frequency measurements are then done. The evaluation of these measurements, however, is performed using a phase correction to account for the Doppler frequency and the phase changes due to the movement of the target between the single measurement steps. As the position of the target is still unknown, and only the radial speed components are known (they add up to different speed vectors for different target locations), a potential speed vector is determined for each cell of the image area, and the imaging algorithm according to (1) is performed including a correction with respect to the assumed speed vector

$$A(P) = \left(r_{1P} \sum_{i=0}^{N-1} \boldsymbol{E}_{i11} \cdot e^{j2k_i r_{1P}} \cdot \underline{\underline{e^{j2\pi f_{D1} \cdot i \cdot \Delta t}}} \right) \cdot \left(r_{2P} \sum_{i=0}^{N-1} \boldsymbol{E}_{i22} \cdot e^{j2k_i r_{2P}} \cdot \underline{\underline{e^{j2\pi f_{D2} \cdot i \cdot \Delta t}}} \right) \cdot \left(\sqrt{r_{1P} \cdot r_{2P}} \sum_{i=0}^{N-1} \boldsymbol{E}_{i12} \cdot e^{jk_i (r_{1P} + r_{2P})} \cdot \underline{\underline{e^{j2\pi f_{DB} \cdot i \cdot \Delta t}}} \right). \quad (2)$$

The correction factors are underlined. f_{D1}, f_{D2}, and f_{DB} are the radial Doppler frequencies with respect to sensors 1 and 2 and the bistatic response, respectively, Δt is the time between the two frequency steps. This correction is valid only if the target is really present in that cell; consequently, only at the real position of the target is amplitude raised.

Fig. 9. Car approaching the sensor from forward left-hand side (distance 17 m, speed 8.1 m/s).

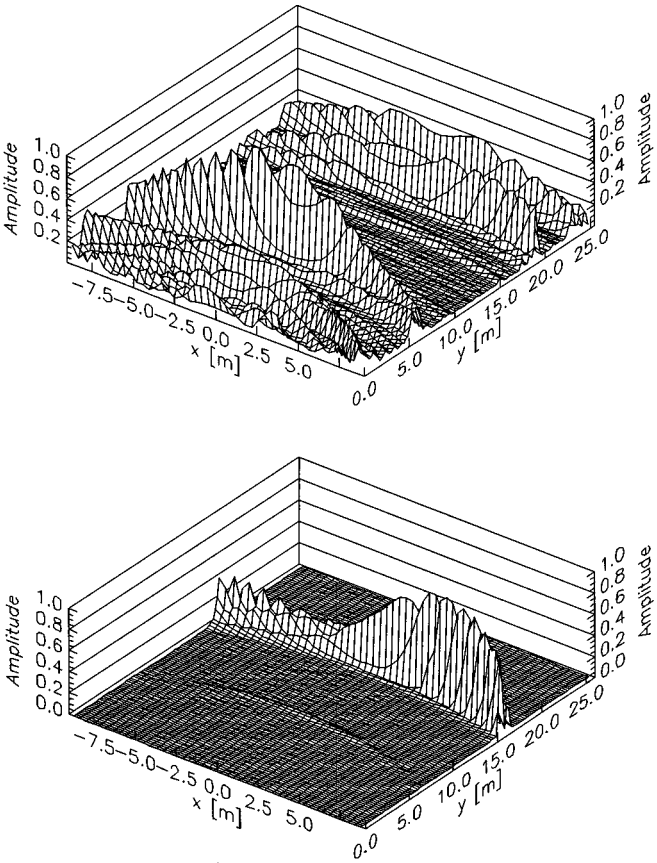

Fig. 10. Uncorrected and corrected radar image of the scene in Fig. 9.

This correction procedure was applied to the data of the above-mentioned moving car. The two corners of the car can now be clearly recognized, i.e., Fig. 8 (bottom). The speed of this car was 1.5 m/s at a distance of 5.5 m.

A second scenario is a car approaching the sensor from a diagonal direction (Fig. 9) at a distance of approximately 18 m and a speed of about 8 m/s. Uncorrected and Doppler corrected data are plotted in Fig. 10. From the uncorrected plot, no relevant information can be gained. After correction, the position of the car becomes visible, although some artifacts show up on the left-hand side. This has to be checked further. From the measurements, a distance of 17 m and a speed of 8.1 m/s could be derived.

VI. Conclusions

The principle of a novel close-range radar sensor for possible applications with small autonomous vehicles or as a automotive sensor for driving backward has been demonstrated in this paper. A mobile test system has been built, and the first results have been shown, including both a stationary and moving target.

References

[1] H. H. Meinel, "Applications of microwaves and millimeter waves for vehicle communications and control in Europe," in *IEEE MTT-S Int. Microwave Symp. Dig.*, Albuquerque, New Mexico, 1992, pp. 609–612.

[2] H. Daembkes and J. F. Luy, "Millimeter-wave components and systems for automotive applications," *Microwave Eng. Europe*, pp. 43–48, Dec.–Jan. 96.

[3] M. Kotaki *et al.*, "Development of millimeter wave automotive sensing technology in Japan," in *IEEE MTT-S Int. Microwave Symp. Dig.*, Albuquerque, 1992, pp. 709–712.

[4] M. Lange *et al.*, "94 GHz imaging radar for autonomous vehicles," in *18th European Microwave Conf.*, Stockholm, Sweden, 1988, pp. 826–830.

[5] A. G. Stove, "80 GHz radar for cars," in *Military Microwave Conf.*, London, U.K., 1992, pp. 389–394.

[6] H. T. Steenstra, F. L. Muller, and P. J. F. Swart, "Multistatic FMCW radar for collision avoidance applications, optimization of the antenna configuration and improving the data processing," in *28th European Microwave Conf.*, vol. II, Munich, Germany, 1999, pp. 13–16.

[7] B. Michael and W. Menzel, "A novel close-range imaging system," in *26th European Microwave Conf.*, Prague, Czech Republic, 1996, pp. 130–134.

[8] F. J. Harris, "On the use of windows for harmonic analysis with the discrete Fourier transform," *Proc. IEEE*, vol. 66, pp. 51–83, Jan. 1978.

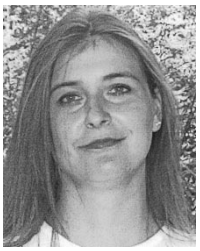

Birgit Michael received the Dipl.-Ing. degree in electrical engineering from the Technical University of Ilmenau, Ilmenau, Germany, in 1991.

From 1991 to 1992, she was with the Department of Microwave Technique, University of Ulm. From 1992 to 1993, she was engaged in the development for multimedia software in a small company. From 1993 to 2000, she rejoined the University of Ulm, as a Research Assistant, where she was engaged in the investigation of a near-range millimeter-wave imaging system. In 2000, she joined the DaimlerChrysler Research Center, Ulm, Germany, where she is currently engaged in research and development of imaging radar systems for obstacle detection.

Wolfgang Menzel (M'89–SM'90) received the Dipl.-Ing. degree from the Technical University of Aachen, Aachen, Germany, in 1974, and the Dr.-Ing. degree from the University of Duisburg, Duisburg, Germany, in 1977.

From 1979 to 1989, he was with the Millimeter-Wave Department, AEG [now European Aerospace and Defense Systems (EADS)], Ulm, Germany. From 1980 to 1985, he was Head of the Laboratory for Integrated Millimeter-Wave Circuits. From 1985 to 1989, he was Head of the Millimeter-Wave Department. During that time, his areas of research included planar antennas, planar integrated circuits, and system in the millimeter-wave frequency range. In 1989, he became a Full Professor at the University of Ulm, Ulm, Germany. His current areas of interest are (multilayer) planar and waveguide circuits, antennas, millimeter-wave interconnects and packaging, and millimeter-wave system aspects.

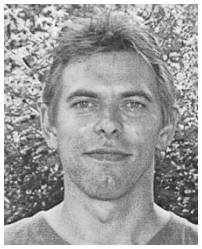

Arnold Gronau received his Diploma degree from the University of Applied Sciences (Fachhochschule), Ulm, Germany, in 1989.

Since 1989, he has been a Member of Technical Staff in the Microwave Department, University of Ulm, Ulm, Germany. His current areas of work include analog and digital circuits and systems and measurement techniques in the area of communication and sensors.